

How short-range attractions impact the structural order, self-diffusivity, and viscosity of a fluid

William Krekelberg*

Department of Chemical Engineering, University of Texas at Austin, Austin, TX 78712.

Jeetain Mittal†

Laboratory of Chemical Physics, NIDDK, National Institutes of Health, Bethesda, MD 20892-0520.

Venkat Ganesan‡ and Thomas M. Truskett§

Department of Chemical Engineering and Institute for Theoretical Chemistry, University of Texas at Austin, Austin, TX 78712.

We present molecular simulation data for viscosity, self-diffusivity, and the local structural ordering of (i) a hard-sphere fluid and (ii) a square-well fluid with short-range attractions. The latter fluid exhibits a region of dynamic anomalies in its phase diagram, where its mobility increases upon isochoric cooling, which is found to be a subset of a larger region of structural anomalies, in which its pair correlations strengthen upon isochoric heating. This “cascade of anomalies” qualitatively resembles that found in recent simulations of liquid water. The results for the hard-sphere and square-well systems also show that the breakdown of the Stokes-Einstein relation upon supercooling occurs for conditions where viscosity and self-diffusivity develop different couplings to the degree of pairwise structural ordering of the liquid. We discuss how these couplings reflect dynamic heterogeneities. Finally, we note that the simulation data suggests how repulsive and attractive glasses may generally be characterized by two distinct levels of short-range structural order.

I. INTRODUCTION

Colloidal fluids play a central role both in technology and in the study of condensed matter. Regarding the latter, suspensions of colloids are interesting model systems because they can behave collectively in ways that are similar to atomic and molecular liquids while simultaneously being both large and slow enough to allow experimental measurements of their real-space structure and dynamics. Despite the similarities between the behaviors of colloids, atoms, and molecules, there also are important, qualitative differences.^{1,2} For example, the effective interparticle attractions between colloids can be “tuned” to be short-ranged relative to the particle diameter σ , unlike the dispersion attractions in atomic and molecular systems that decay more gradually with interparticle separation r , i.e., as $(\sigma/r)^{-6}$.

Short-ranged attractive (SRA) interactions have nontrivial implications for the static structural, equilibrium thermodynamic, and dynamic behaviors of colloidal suspensions. For instance, whereas cooling a simple atomic liquid generally slows down its dynamic processes, several recent studies have demonstrated that reducing the temperature (or increasing the attractive interactions) of an SRA fluid can have a non-monotonic effect on its mobility. In fact, concentrated SRA fluids can vitrify not only upon cooling, forming an “attractive” glass or gel, but also upon heating, forming a “repulsive” or hard-sphere (HS) glass.^{2,3,4,5,6,7,8} Since the structural and mechanical properties of these glassy states can be quite different, there is a broad interest in understanding the properties of the precursor supercooled fluids from which they are formed.

In this article, we explore whether the unusual effect that temperature has on the dynamics of SRA fluids reflects a more general connection between the static structure and the dynamics of condensed phases. In doing so, we find it instruc-

tive to view the behavior of SRA fluids in the context of another well-studied system with anomalous dynamical trends, liquid water. Cold water behaves differently than simple fluids in that its mobility *increases* upon isothermal compression over a broad range of conditions. Interestingly, the state points where water shows this behavior is a subset of a larger region on its phase diagram where its local structural order anomalously *decreases* upon compression.^{9,10} In other words, there is a “cascade of anomalies”⁹ where the pressure-induced disordering of liquid water emerges at a lower density, and ultimately disappears at a higher density, when compared to the pressure-induced increase in its mobility. It has been recently argued^{11,12,13} that this behavior follows from the fact that water approximately obeys a scaling relationship between its self-diffusivity and the structural order parameter $-s_2/k_B$, where s_2 is the contribution to the fluid’s excess entropy due to its static oxygen-oxygen pair correlations, and k_B is the Boltzmann constant.

Here, we use molecular dynamics simulations to systematically investigate the relationships between static structural order ($-s_2/k_B$), self-diffusivity (D), and viscosity (η) for both a HS fluid and an SRA fluid. One of our main aims is to understand whether the latter shows a cascade of anomalies similar to that of liquid water. Specifically, we are interested in whether the region on the phase diagram of an SRA fluid where it becomes more mobile (higher D , lower η) upon cooling is a subset of a larger set of conditions where the fluid becomes more ordered (higher $-s_2/k_B$) upon heating. A second, and related, goal of this study is to explore whether the relationships between D , η , and $-s_2/k_B$ can provide generic insights into the breakdown of the Stokes-Einstein (SE) relation ($D\eta/T \approx \text{constant}$) in deeply supercooled liquids and also into the structural properties of repulsive and attractive glasses.

The organization of the paper is as follows. In Section II,

we describe the two model systems examined in this study and also the simulation methods used to carry out the investigation. Then, in Section III, we present our simulation results and discuss their relevance for understanding the connection between structural order and mobility in HS and SRA fluids. Finally, in Section IV, we present some concluding remarks.

II. MODELING AND SIMULATION

We focus on two model systems: a fluid of HS particles and a fluid of square-well particles with short-range attractions, the latter of which we denote the SW-SRA fluid. The interparticle potential $\mathcal{V}(r_{12})$ between particles 1 and 2 for these systems is given by

$$\mathcal{V}(r_{12}) = \begin{cases} \infty & r_{12} \leq \sigma_{12}, \\ -\epsilon & \sigma_{12} < r_{12} < \lambda\sigma_{12}, \\ 0 & r_{12} \geq \lambda\sigma_{12}. \end{cases} \quad (1)$$

where r_{12} is the distance between the particle centers, $\sigma_{12} = (\sigma_1 + \sigma_2)/2$ is the interparticle diameter, and the parameters ϵ and λ set the magnitude and range of the interparticle attraction, respectively. For the HS fluid, one has $\lambda = 1$, and thus there are no interparticle attractions. We choose $\lambda = 1.03$ for the SW-SRA fluid, a range similar to that of other SW-SRA fluids known to exhibit anomalous dynamical behavior^{8,14}. In order to avoid crystallization in our study, and thus allow study of the supercooled fluid states, we have drawn the individual particle diameters σ_i of both systems from a Gaussian distribution with an average of σ and standard deviation of $s = 0.1\sigma$. For practical reasons, we truncated this distribution so that all particle diameters lie in the range $\sigma - 3s \leq \sigma_i \leq \sigma + 3s$. We have implicitly non-dimensionalized all reported quantities in this investigation by appropriate combinations of the characteristic length scale, $l_c = \sigma$ and a model-dependent time scale τ_c . For the HS fluid, the characteristic time scale τ_c is cast in terms of the temperature $\tau_c = \sqrt{m\sigma^2/k_B T}$, where m is the particle mass, while for the SW-SRA fluid it is defined in terms of the attractive strength of the potential, $\tau_c = \sqrt{m\sigma^2/\epsilon}$.

To explore the behavior of these model systems, molecular dynamics simulations were performed using an event-driven algorithm¹⁵ in the microcanonical ensemble. For all runs, $N = 1000$ particles were simulated in a cubic simulation cell of volume V with periodic boundary conditions. Particle packing fractions $\phi_c = \pi \sum \sigma_i^3 / (6V)$ in the range $0.35 \leq \phi_c \leq 0.6$ were investigated for both model systems, and temperatures T in the range $0.3 \leq T \leq 2.0$ were examined for the SW-SRA fluid. For each thermodynamic state point, between three and ten independent simulations were performed in order to estimate the errors in the transport coefficients. Self-diffusivities D were calculated by fitting the long time ($t \gg 1$) mean-squared displacements to the Einstein relation for self-diffusivity $\langle \delta r^2 \rangle = 6Dt$. Zero-shear viscosities were calculated using the impulse limit of the Einstein formula.¹⁶ The structural order parameter $-s_2$ was computed

using the expression

$$-s_2 = \frac{\rho}{2} \int \{g(\mathbf{r}) \ln g(\mathbf{r}) - [g(\mathbf{r}) - 1]\} d\mathbf{r}, \quad (2)$$

where $\rho = N/V$ is the number density, and $g(\mathbf{r})$ is the average pair correlation function. Note that $-s_2 = 0$ for an ideal gas, and $-s_2 \rightarrow \infty$ for a perfect crystalline lattice. Thus, as has been discussed at length elsewhere^{11,12,17}, one can view $-s_2$ as a scalar measure of the amount of pair-wise translational order of the system.

III. RESULTS AND DISCUSSION

A. Transport and Structural Properties

We now examine some of the state-dependent transport and structural properties of the HS and SW-SRA fluids. For the HS fluid, the quantities D , η , and $-s_2$ (non-dimensionalized as outlined in Section II) depend only on the packing fraction ϕ_c , whereas the corresponding dimensionless properties for the SW-SRA fluid depend on both packing fraction ϕ_c and temperature T .

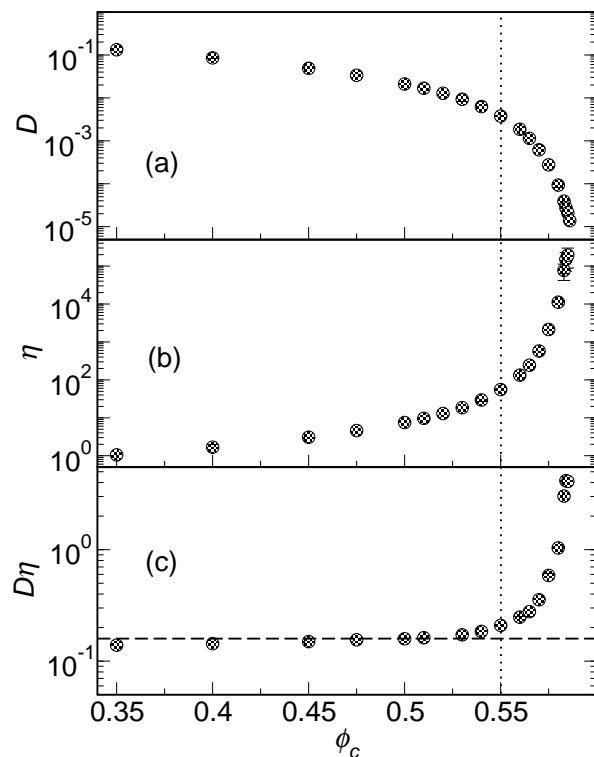


FIG. 1: Transport properties of the HS fluid described in the text as a function of packing fraction ϕ_c : (a) self-diffusivity D , (b) viscosity η , and (c) SE relationship $D\eta/T$. The horizontal dashed line in (c) indicates $(2\pi)^{-1}$, the expected value of the SE relation in the slip limit, and the vertical line denotes the point at which $D\eta = 1.2/(2\pi)$. In this work, we use this simple heuristic to identify the breakdown of the SE relation.

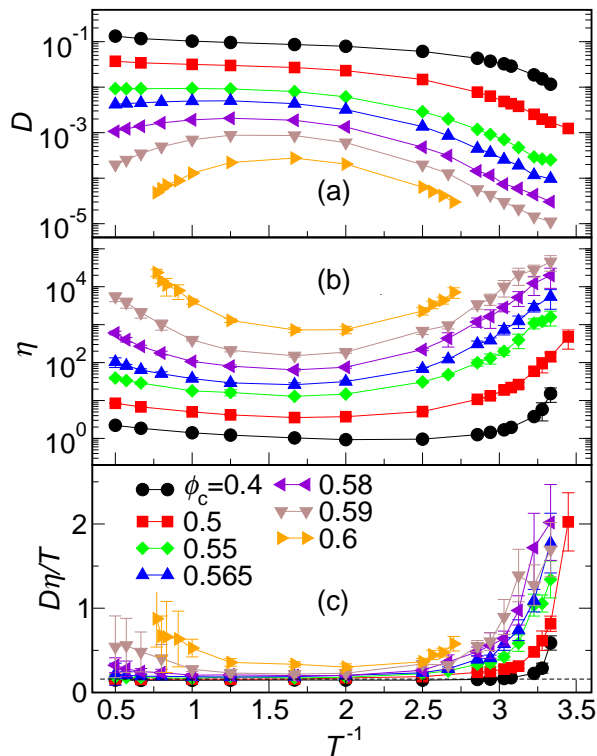


FIG. 2: Transport properties of the SW-SRA fluid described in the text as a function of packing fraction ϕ_c and reciprocal temperature T^{-1} : (a) self-diffusivity D , (b) viscosity η , and (c) SE relationship $D\eta/T$. The horizontal dashed line in (c) indicates $(2\pi)^{-1}$, the expected value of the SE relation in the slip limit.

The transport properties of the HS fluid are displayed in Fig. 1. As expected, with increasing packing fraction ϕ_c , the self-diffusivity D monotonically decreases, while the viscosity η monotonically increases. The changes in both of these properties become more pronounced for $\phi_c > 0.55$, conditions for which $D(\phi_c)$ can be accurately fitted using either Vogel-Fulcher or power-law functional forms¹⁸ with a predicted divergence near $\phi_c \sim 0.6$.

Figure 1(c) illustrates that the SE relation in the slip limit, $D\eta \approx (2\pi)^{-1}$, is approximately obeyed by this HS fluid for $\phi_c < 0.55$. However, for higher packing fractions, large positive deviations from the slip limit of the SE relation become apparent.¹⁸ This type of SE “breakdown” has been observed in studies of several glass-forming fluids in their deeply supercooled states.^{19,20,21,22}

We note that, as observed by previous investigators,¹⁸ the SE relation is not strictly obeyed by the HS fluid even at lower packing fractions. For example, the product $D\eta$ varies by approximately 30% as the packing fraction is increased from $\phi_c = 0.35$ to 0.55. However, the breakdown of the SE relation is typically understood to occur when the product begins to exhibit a pronounced positive deviation from the slip value. In this work, we identify the breakdown of the SE relation by the heuristic criterion, $D\eta \geq 1.2/(2\pi)$. As can be seen from Figure 1(c), this threshold is crossed at $\phi_c \approx 0.55$ for the HS fluid investigated here.

The simulated transport properties of the SW-SRA fluid are displayed in Fig. 2 as a function of reciprocal temperature T^{-1} along isochores. The most striking feature of this plot is that D exhibits a maxima with inverse temperature, a behavior that has also been observed in both experiments and computer simulations of other SRA fluids.^{3,4,5,6,7,8,23,24,25} As discussed in Section I, this trend becomes pronounced at high ϕ_c , where the system can ultimately form either a repulsive glass by isochoric heating or an attractive glass or gel via isochoric cooling.

The behavior of the zero-shear viscosity η of the SW-SRA fluid, displayed in Fig. 2(b), qualitatively mirrors that of its self-diffusivity. For a more quantitative comparison, the SE relationship $D\eta/T$ is plotted in Figure 2(c). Note that the slip limit of the SE relation is again approximately obeyed for the SW-SRA fluid over a broad range of T^{-1} and ϕ_c . However, for all values of ϕ_c investigated here, the SE relation breaks down at sufficiently low T , as the attractive glass transition is approached. At high T , on the other hand, only the highest ϕ_c isochore studied showed a significant breakdown of the SE relation. This asymmetry between high and low T behaviors has also been observed in other model SRA fluids.^{8,14,23,24} It simply reflects the fact that one must reach a relatively high value of ϕ_c in these systems to achieve the level of frustration required to form a repulsive glass, whereas interparticle attractions can induce formation of the attractive glass at much lower particle concentrations.

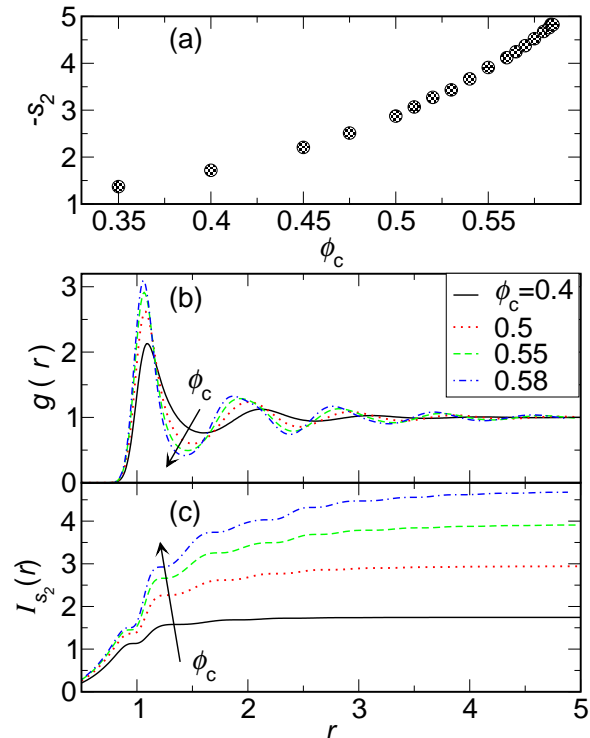


FIG. 3: Structural properties of the HS fluid discussed in the text. (a) Translational structural order parameter $-s_2$ versus packing fraction ϕ_c . (b) Radial distribution function $g(r)$ for several packing fractions. (c) Cumulative order integral (see Eq. 3). Arrows indicate increasing ϕ_c .

It is natural to wonder whether the decrease in mobility that the HS and SW-SRA fluids experience upon approach to the glass transition is generally correlated with an increase in the amount of local structural order that they exhibit. To explore this issue, we first examine the behavior of the structural order parameter $-s_2$ for the HS fluid. As can be seen in Fig. 3(a), $-s_2$ for this system monotonically increases with packing fraction, indicating a strengthening of the pair-wise interparticle correlations. From the radial distribution functions $g(r)$ shown in Fig. 3(b), it is also evident that these correlations correspond to the progressive development of well-defined coordination shells around the particles. The contributions of these shells to the translational order parameter $-s_2$ become readily apparent when we investigate the following cumulative order integral,

$$I_{s_2}(r) = 2\pi\rho \int_0^r r'^2 \{g(r') \ln g(r') - [g(r') - 1]\} dr'. \quad (3)$$

Note that one recovers $-s_2$ from this integral in the large r limit, and thus $I_{s_2}(r)$ quantifies the average amount of translational ordering on length scales smaller than r surrounding a particle. In Fig. 3(c), we observe nearly step-wise increases in $I_{s_2}(r)$ at the locations of the various coordination shells. It is also clear that increasing ϕ_c of the HS fluid has two main effects on its structural order. It strengthens the ordering within the individual coordination shells, and it uniformly increases the number of coordination shells (i.e., the range of order).

The behavior of the structural order parameter $-s_2$ for the SW-SRA fluid is displayed in Fig. 4(a) as a function of reciprocal temperature T^{-1} along isochores. In accord with what might be expected based on the behavior of this fluid's transport coefficients, $-s_2(T)$ displays broad minima. At low T , heating the fluid decreases its structural order (similar to what happens in normal molecular fluids), but, at high T , heating anomalously increases its structural order.

To determine the origins of this trend, we focus on the behaviors of the radial distribution function and the cumulative order integral for the SW-SRA fluid along the $\phi_c = 0.55$ isochore. As can be seen in Fig. 4(b)-(e), heating induces subtle changes in $g(r)$ that result in nontrivial cumulative changes in the structural order. In particular, heating the cold fluid ($T \leq 0.4$) results in a barely detectable decrease in the height of the first peak of $g(r)$, and it has little effect on the other coordination shells. However, as is shown in Fig. 4(c), even these subtle modifications to $g(r)$ result in significant changes to the cumulative order integral of the fluid. In particular, heating the cold fluid decreases the total amount of pair-wise structural order, even though the range of the order remains essentially the same. This change is qualitatively consistent with the thermal weakening of transient clustered configurations of physically “bonded” particles observed in SRA fluids at lower temperatures.^{2,25,26,27}

The effect of increasing temperature on the structure of the warm SW-SRA fluid ($T > 0.4$) is different [see Fig. 4(d) and (e)]. In particular, heating continues to decrease the height of the first peak in $g(r)$, but it also broadens the peak and enhances the interparticle correlations associated with the other,

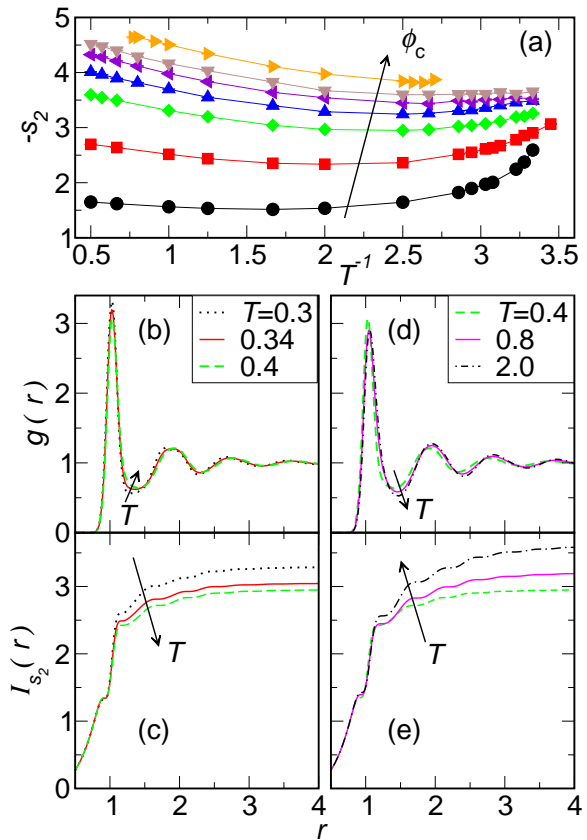


FIG. 4: Structural properties of the SW-SRA fluid. (a) Structural order parameter $-s_2$ versus reciprocal temperature T^{-1} . Symbols are the same as in Fig. 2. (b) Radial distribution function $g(r)$ and (c) cumulative order integral $I_{s_2}(r)$ for $\phi_c = 0.55$ and $T \leq 0.4$. (d) Radial distribution function $g(r)$ and (e) cumulative order integral $I_{s_2}(r)$ for $\phi_c = 0.55$ and $T \geq 0.4$.

more distant, coordination shells. The net effect is an *increase* in both the total amount of translational structural order and its range. This structural change is due to the fact that heating the warm fluid collapses the open channels of free volume that form at intermediate T due to weak interparticle clustering,²⁷ essentially jamming the particles into a less efficient, and more correlated, packing arrangement.^{2,4,8,27}

It is clear from the results presented in this section that there is a qualitative (negative) correlation between pair-wise structural order and mobility in both the HS and SW-SRA fluids. In the following two sections, we explore the extent to which this connection can be made quantitative.

B. Connection between structure and mobility anomalies

As discussed in Section III A, at high T and ϕ_c , both the self-diffusivity and the structural order of the SW-SRA fluid behave in a manner that is anomalous when compared to simple molecular fluids [see Figs. 2(a) and 4(a)]. Whereas increasing T of a simple fluid generally increases its mobility, isochorically heating the warm SW-SRA fluid can result in

slower single-particle dynamics. This latter behavior is characterized by the following inequality:

$$\left(\frac{\partial D}{\partial T}\right)_{\phi_c} < 0, \quad \text{self-diffusivity anomaly.} \quad (4)$$

The structural order of a simple molecular fluid, on the other hand, normally decreases when it is isochorically heated. Therefore, we denote conditions for which the following inequality holds (i.e., order increases upon heating),

$$\left(\frac{\partial[-s_2]}{\partial T}\right)_{\phi_c} > 0, \quad \text{structural anomaly,} \quad (5)$$

as “structurally anomalous”.

The locations of the regions for self-diffusivity and structural anomalies of the SW-SRA fluid in the T - ϕ_c plane, as determined by numerical differentiation of the data in Figs. 2(a) and 4(a), respectively, are displayed in Fig. 5(a). A schematic based on the data is provided in Fig. 5(b). The most striking point is that the region of structural anomalies appears to completely envelop the region of self-diffusivity anomalies. In other words, the SW-SRA fluid exhibits unusual T -dependencies for its single-particle dynamics only for those state points where it also exhibits unusual T -dependencies for its structural order.

This “cascade” of structural and dynamic anomalies shown by the SW-SRA fluid is very similar to that observed originally in simulations of the SPC/E model of water⁹ and later in simulations of other simpler models that also show water-like behavior.^{12,28,29,30,31} Recall that cold water behaves differently from simple fluids over a wide range of conditions in that its mobility increases, while its structural order decreases, when it is isothermally compressed. Thus, the generic similarity between the behavior of water and the SW-SRA fluid shown in Fig. 5 is that, in both cases, the region on the phase diagram where mobility anomalies occur is a subset of the region where structural anomalies are found. It has been recently argued^{11,12,13} that this type of behavior for water follows directly from the fact that liquid water approximately obeys a scaling relationship between its self-diffusivity and its translational structural order parameter $-s_2$ over a wide range of temperature and density. In the next section, we test whether there exist similar scaling relations between $-s_2$ and the transport coefficients of the HS and SW-SRA fluids. We also discuss how such relations might provide insights into the breakdown of the SE relation for these systems.

C. Structure-property relations and the breakdown of Stokes-Einstein

As alluded to above, recent molecular dynamics simulations¹¹, motivated by other earlier observations of Rosenfeld^{32,33} and Dzugasov³⁴, have demonstrated that the following simple relation is approximately obeyed by various

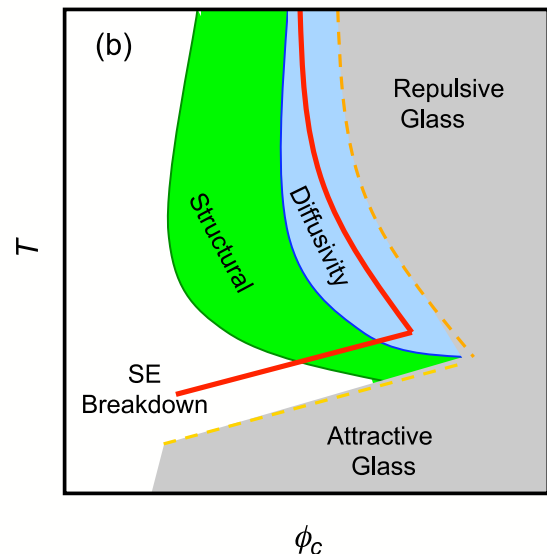
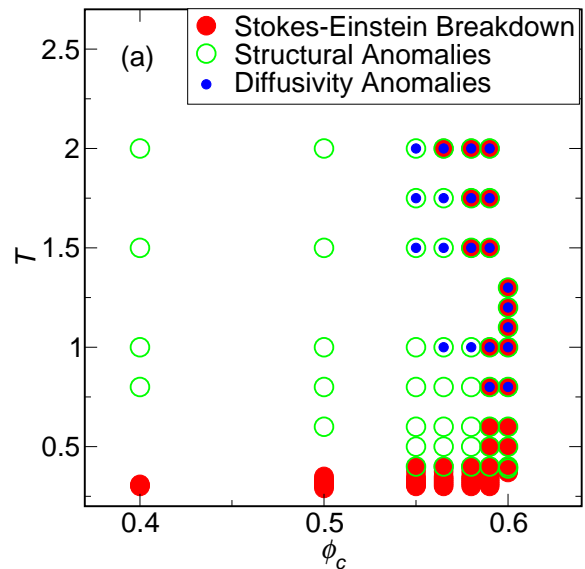


FIG. 5: Conditions exhibiting self-diffusivity and structural anomalies, as well as breakdown of the SE relation [$D\eta/T > 1.2/(2\pi)$, see discussion in text] for the SW-SRA fluid in the T - ϕ_c plane. (a) Results from simulations. Large closed circles are state points where the SE relationship breaks down. Open circles represent the region of structural anomalies defined by Eq. (5). Small closed circles represent the region of self-diffusivity anomalies defined by Eq. (4). (b) Schematic representation of the data. The green shaded region (and area to its right) represents state points where the fluid is structurally anomalous. The blue shaded region represents state points exhibiting the self-diffusivity anomaly. Points to the right of the red curve show a breakdown of the SE relation. The gray region represents the repulsive and attractive glassy states.

model fluids in their equilibrium liquid states:

$$D = A_D \exp[B_D s_2], \quad (6a)$$

where A_D and B_D are parameters which may depend on packing fraction (i.e., density), but not on T . Results from other earlier theoretical studies,³² and considerations based on the Stokes-Einstein relation, suggest that a similar relationship should approximately hold for the zero-shear viscosity η of these equilibrium fluids:

$$\eta = A_\eta \exp[B_\eta s_2] \quad (6b)$$

where, again, A_η and B_η may depend on packing fraction (density) only.

However, given that the SE relation breaks down as a liquid is supercooled, it is apparent that Eq. (6a) and (6b), with coefficients fit to higher temperature equilibrium fluid data, cannot also describe the transport coefficients in deeply supercooled liquid states. Nonetheless, it has recently been shown that the functional form of Eq. (6a) can in fact approximately describe the isochoric self-diffusivity data of model supercooled liquids over a broad range of temperatures if a different pair of parameters A'_D and B'_D are adopted.¹¹ In other words, there appears to be a crossover upon cooling where the self-diffusivities of fluids transition from being approximately described by $D = A_D \exp[B_D s_2]$ for equilibrium states to being approximately described by $D = A'_D \exp[B'_D s_2]$ for supercooled conditions. Of course, even this latter relation must eventually fail for conditions very near the glass transition where both D and η^{-1} rapidly vanish, while s_2 remains finite.¹⁷ We will return to this last point at the end of the section.

The structure-property scalings discussed above suggest several interesting questions concerning the liquid state. For example, does the aforementioned crossover between scaling relations occur near the breakdown of the SE relation? Furthermore, does a similar crossover for the s_2 dependence of η occur upon supercooling? If so, does it coincide with the crossover point for D ? Below, we use our molecular dynamics simulation results to investigate these questions for the HS and SW-SRA fluids. The idea is that the new information that we gain about how D and η couple to pair structure should give insights into the SE breakdown and the general effects that supercooling has on liquids.

First, we consider the HS fluid. Figure 6 displays the transport coefficients and the SE relationship for this system as a function of the structural order parameter, $-s_2$, which itself depends only on packing fraction ϕ_c . Although the basic scaling relations outlined above describe the behavior of attractive fluids along isochores, they apply equally well for athermal fluids (such as this) along isotherms, keeping in mind that the glass transition in the latter is approached by compression and not by cooling. One important aspect to note in Fig. 6 is that there is, in fact, a crossover between “equilibrium” (low $-s_2$) and “supercooled” (high $-s_2$) states. In fact, Eq. (6) provides a quantitative fit to the data for packing fractions in the range $0.35 < \phi_c < 0.55$ ($1.4 < -s_2 < 3.9$). Interestingly, the point at which both transport coefficients diverge from this equilibrium scaling relationship closely coincides with the packing fraction ($\phi_c \approx 0.55$) where $D\eta = 1.2/(2\pi)$, i.e., the breakdown of the SE relation.

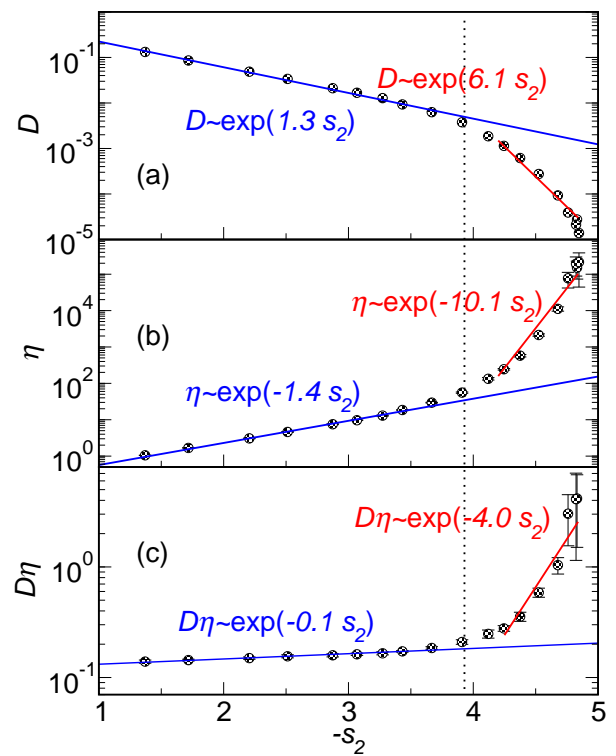


FIG. 6: Transport properties as a function of structural order parameter $-s_2$ for the HS fluid described in the text. (a) Self-diffusivity D , (b) viscosity η , and (c) the SE relationship. In (a) and (b), the blue and red lines represent fits to Eq. 6 for the equilibrium and supercooled states, respectively.

It is also evident from Fig. 6 that one can use the scaling form of Eq. (6) with different pairs of coefficients to approximately describe the s_2 dependencies of the transport coefficients for the supercooled HS fluid. The fits of Eq. (6) for these supercooled states, however, are not as accurate as those for the equilibrium fluid data below the crossover. In fact, our only goal in fitting the supercooled liquid data to this exponential form is that it allows us to extract simple quantitative measures [B'_D and B'_η] of the couplings that exist between the transport coefficients and the static structure of the fluid. It can be seen both from the raw data in Fig. 6 and from the values of these coefficients for the “equilibrium” and “supercooled” HS fluid [$(B_D = 1.3, B_\eta = -1.4)$ and $(B'_D = 6.1, B'_\eta = -10.1)$, respectively] that the breakdown of the SE relation coincides with qualitative change in how static structure correlates to D and η . In the equilibrium fluid, both transport coefficients show weak, and roughly equivalent, couplings to s_2 . However, after the SE breakdown, the transport coefficients develop much stronger couplings to structural order. This is presumably due to the integral role that cooperative structural rearrangements play in the relaxation of deeply supercooled liquids.³⁵

It is clear from Fig. 6 that the reason that the SE relation breaks down in this system is because the viscosity of the deeply supercooled HS fluid becomes much more sensitive to changes in static structural order than the self-diffusivity. This

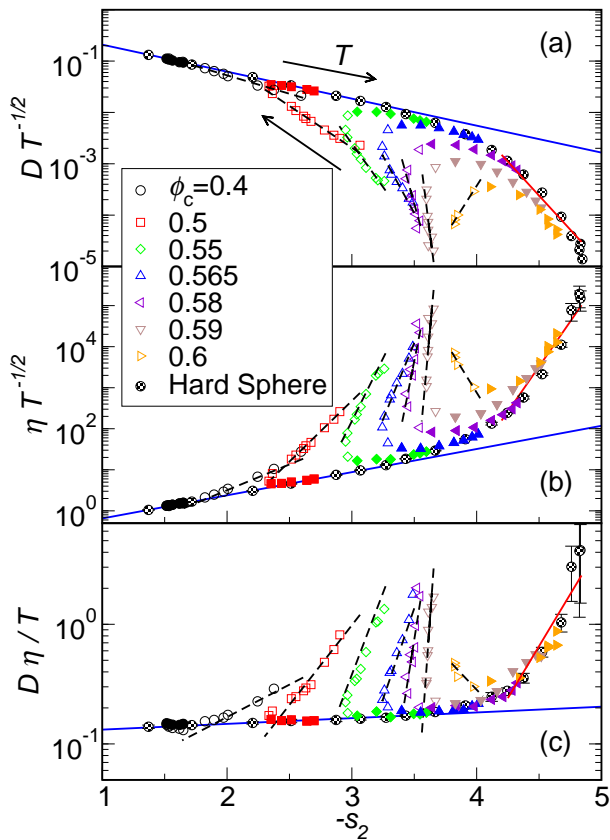


FIG. 7: (a) Scaled self-diffusivity $DT^{-1/2}$, (b) scaled viscosity $\eta T^{-1/2}$, and (c) SE relationship $D\eta/T$ versus structural order parameter $-s_2$ for the SW-SRA fluid at several packing fractions ϕ_c . Self-diffusivity D , viscosity η , and the SE relationship $D\eta$ for the HS fluid are provided for comparison. Filled and open symbols represent the high ($T > 0.5$) and low ($T < 0.5$) temperature branches of the SW-SRA fluid, respectively. Dashed lines in (a) and (b) are fits of the SW-SRA data to Eq. (6) and the dashed lines in (c) are the products of the respective fits in (a) and (b). Arrows in (a) indicate the general direction of increasing T . Red and blue lines have the same meaning as those in Fig. 6.

is consistent with the observations of previous studies that have correlated the breakdown of the SE relationship to the onset of heterogeneous dynamics.^{18,36,37,38,39} Heterogeneous dynamics is typically characterized by the presence of many particles that transiently exhibit exceedingly high or low values mobility relative to the mean. The highly mobile particles have been shown to readily diffuse distances on the order of a particle diameter by so-called “hopping” motions. It is presumably the presence of these highly mobile particles that allows the self-diffusivity to maintain a weaker coupling to static structure than the viscosity.

Displayed in Fig. 7 are the scaled transport coefficients, $DT^{-1/2}$ and $\eta T^{-1/2}$, of the SW-SRA fluid as a function of the structural order parameter $-s_2$. The $T^{-1/2}$ factor is included here to remove the trivial “thermal velocity” contribution to these transport coefficients, which then allows them to be directly compared to the dimensionless values of D and η of the HS fluid. Along these lines, it should be noted that

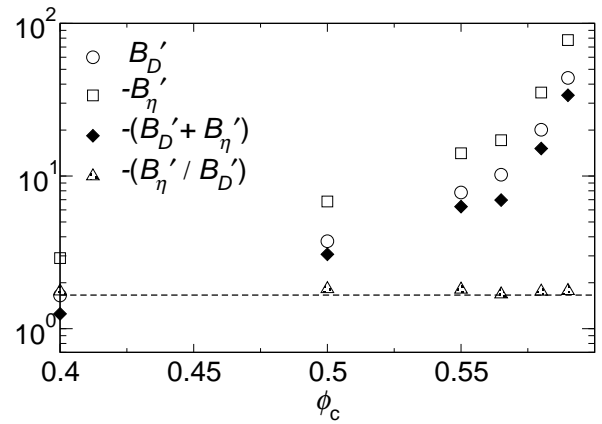


FIG. 8: Values of the coupling coefficients B'_D and $-B'_\eta$ from fits of the supercooled SW-SRA data to Eq. (6) (shown in Fig. 7) for the self-diffusivity D and viscosity η , respectively. Also shown are the (negative) sum $-(B'_D + B'_\eta)$ and the ratio $-(B'_\eta / B'_D)$ of the exponents. The dashed line represents the HS fluid value for $-(B'_\eta / B'_D)$.

the high temperature data points for $DT^{-1/2}$, $\eta T^{-1/2}$, and $D\eta/T$ of the SW-SRA fluid ($T > 0.5$, denoted in Fig. 7 by filled symbols) are indeed approximately described by the corresponding data for D , η and $D\eta$ of the HS fluid. One consequence of this is that the breakdown of the SE relation for the SW-SRA fluid upon approaching the repulsive glass transition by heating occurs at approximately the same value of $-s_2$ as the breakdown of the SE relation for the HS fluid upon compression. In contrast, the value of $-s_2$ of the SW-SRA fluid at the breakdown of the SE relation upon cooling toward the attractive glass is different for each packing fraction studied. As might be expected, fluids with lower packing fractions show departures from the slip limit of the SE relation for conditions where they exhibit lower amounts of translational structural order.

Do the SW-SRA transport coefficients also follow “equilibrium” and “supercooled” exponential scaling branches when plotted versus $-s_2$? For $\phi_c < 0.55$ and intermediate temperatures, the data approximately collapse onto the same exponential scaling relation obtained from the fit of the equilibrium HS fluid data (shown in all panels of Fig. 7 as a blue line). At sufficiently high or low temperatures, however, the SW-SRA data transitions to “supercooled” exponential scalings with different coupling coefficients B'_D and B'_η . Interestingly, these transitions closely coincide with the breakdown of the SE relation. In all cases, similar to the HS fluid, D exhibits a considerably weaker dependence on $-s_2$ than does η (i.e., $-B'_\eta > B'_D$, see Fig. 8) after the SE breakdown. Although the difference between the coupling coefficients increases with ϕ_c , the relative magnitude remains approximately constant ($-B'_\eta / B'_D \sim 1.7$) and very similar to that of the HS fluid. This latter structure-property connection is general in the sense that it approximately holds for these model liquids as they become “supercooled” via heating, cooling, or compression.

We would like to conclude this section with a speculation. Although it is not yet possible to equilibrate molecular dynam-

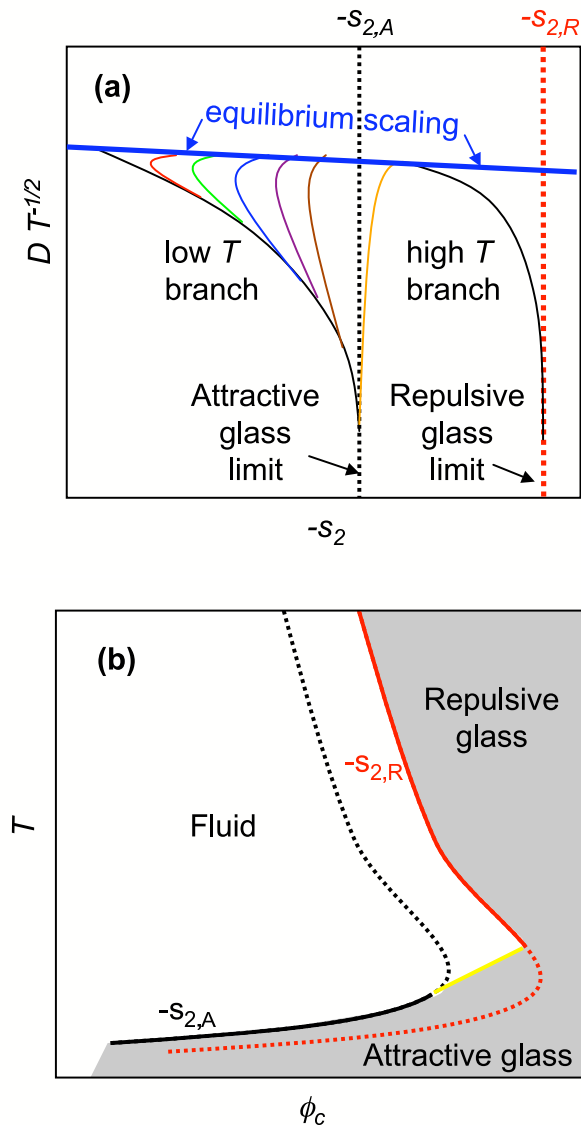


FIG. 9: (a) Schematic representing a speculation about how the scaled self-diffusivity vs $-s_2$ isochores of the SW-SRA fluid [Fig. 7(a)] might behave as the repulsive and attractive glass transitions are approached. The quantities $s_{2,R}$ and $s_{2,A}$ represent the limiting values of s_2 for the repulsive and attractive glasses, respectively. (b) The black and red curve are the proposed $\text{iso-}s_2$ loci in the $T - \phi_c$ plane at the characteristic repulsive and attractive glass values, respectively (discussed in the text). The portions of these lines that are solid represent the hypothesized glass transition. The yellow line is a narrow transition region where the glass line is proposed to cross between the $\text{iso-}s_2$ curves.

ics simulations very close to the repulsive or attractive glass transitions in the SW-SRA fluid, the data shown in Fig. 7(a) and (b) are suggestive of what may happen to the structural order of the fluid in those limits. As discussed earlier, the high temperature behaviors of the SW-SRA transport coefficients, when plotted versus $-s_2$, approximately follow the trends of

the HS fluid. Therefore, it is reasonable to suspect that the structural order parameter of the high temperature (repulsive) glass $-s_{2,R}$ will be close to that of the HS glass [Fig. 9(a)]. At low temperatures, the transport coefficients of the SW-SRA fluid as a function of $-s_2$ also appear as if they may asymptote to a different, lower, limiting value [Fig. 9(a)], i.e., a value of the structural order parameter $-s_{2,A}$ characteristic of the attractive glass. The resulting picture is that the repulsive and attractive glass lines closely follow two “ $\text{iso-}s_2$ ” curves, with a sharp transition between the two in a narrow temperature range, shown schematically in Fig. 9(b)). Since s_2 can be readily obtained from static pair correlations, this is a speculation that could be tested via experiments of SRA colloidal fluids.⁴⁰ It would also be interesting to explore in future studies the extent to which liquid-state (e.g., mode-coupling) theories for SRA fluids are able to reproduce the empirical connection between s_2 and dynamics found in our simulations and to test the predictions that they make about how the structural order varies along the ideal repulsive and attractive glass lines.

IV. CONCLUSIONS

We have presented new molecular simulation data for viscosity, self-diffusivity, and the local structural ordering of both a hard-sphere fluid and a square-well fluid with short-range attractions (relative to the particle diameter). We found that the latter system has a region of mobility anomalies in the temperature-packing fraction plane, where its self-diffusivity increases upon isochoric cooling. This region is entirely enclosed within a wider set of state points where the fluid’s pair correlations strengthen upon isochoric heating. This type of “cascade of anomalies” is very similar to that found in recent simulations of liquid water, and it follows from a broader connection between static structure and dynamics in condensed phase systems.

Both the hard-sphere and square-well fluids show that the breakdown of the Stokes-Einstein relation upon supercooling occurs for conditions where viscosity and self-diffusivity develop different couplings to the degree of pairwise structural ordering of the liquid. We discussed how these couplings reflect dynamic heterogeneities. Finally, we provided an experimentally testable hypothesis about how repulsive and attractive glasses may be generally characterized by two distinct levels of short-range structural order. In future work, we will investigate whether there are similar connections between non-equilibrium dynamics (e.g. shear-dependent viscosity) and structural order in these systems.

Acknowledgments

WPK acknowledges financial support of the National Science Foundation for a Graduate Research Fellowship. TMT acknowledges financial support of the National Science Foundation (CTS 0448721), the David and Lucile Packard Foundation, and the Alfred P. Sloan Foundation. VG acknowledges financial support of the Robert A. Welch Foundation and the

Alfred P. Sloan Foundation. Computer simulations for this study were performed at the Texas Advanced Computing Cen-

ter (TACC).

-
- * Electronic address: krekel@che.utexas.edu
 † Electronic address: jeetain@helix.nih.gov
 ‡ Electronic address: venkat@che.utexas.edu
 § Electronic address: truskett@che.utexas.edu; Corresponding Author
- ¹ W. B. Russel, D. A. Saville, and W. R. Schowalter, *Colloidal Dispersions* (Cambridge University Press, New York, 1989).
 - ² F. Sciortino, *Nat. Mater.* **1**, 145 (2002).
 - ³ T. Eckert and E. Bartsch, *Phys. Rev. Lett.* **16**, 125701 (2002).
 - ⁴ K. N. Pham, A. M. Puertas, J. Bergholtz, S. U. Egelhaaf, A. Moussaïd, P. N. Pusey, A. B. Schofield, M. E. Cates, M. Fuchs, and W. C. K. Poon, *Science* **296**, 104 (2002).
 - ⁵ J. Bergholtz and M. Fuchs, *Phys. Rev. E* **59**, 5706 (1999).
 - ⁶ L. Fabbian, W. Gotze, F. Sciortino, P. Tartaglia, and F. Thiery, *Phys. Rev. E* **59**, R1347 (1999).
 - ⁷ K. Dawson, G. Foffi, M. Fuchs, W. Gotze, F. Sciortino, M. Sperrl, P. Tartaglia, T. Voigtmann, and E. Zaccarelli, *Phys. Rev. E* **63**, 011401 (2001).
 - ⁸ E. Zaccarelli, G. Foffi, K. A. Dawson, S. V. Buldyrev, F. Sciortino, and P. Tartaglia, *Phys. Rev. E* **66**, 041402 (2002).
 - ⁹ J. R. Errington and P. G. Debenedetti, *Nature* **409**, 318 (2001).
 - ¹⁰ S. Sastry, *Nature* **409**, 300 (2001).
 - ¹¹ J. Mittal, J. Errington, and T. Truskett, *J. Phys. Chem. B* **110**, 18147 (2006).
 - ¹² J. R. Errington, T. M. Truskett, and J. Mittal, *J. Chem. Phys.* **125**, 244502 (2006).
 - ¹³ R. Sharma, S. N. Chakraborty, and C. Chakravarty, *J. Chem. Phys.* **125**, 204501 (2006).
 - ¹⁴ G. Foffi, K. A. Dawson, S. V. Buldyrev, F. Sciortino, E. Zaccarelli, and P. Tartaglia, *Phys. Rev. E* **65**, 050802(R) (2002).
 - ¹⁵ D. C. Rapaport, *The Art of Molecular Dynamic Simulation* (Cambridge University Press, Cambridge, 2004), 2nd ed.
 - ¹⁶ B. J. Alder, D. M. Gass, and T. E. Wainwright, *J. Chem. Phys.* **53**, 3813 (1970).
 - ¹⁷ T. M. Truskett, S. Torquato, and P. G. Debenedetti, *Phys. Rev. E* **62**, 993 (2000).
 - ¹⁸ S. K. Kumar, G. Szamel, and J. F. Douglas, *J. Chem. Phys.* **124**, 214501 (2006).
 - ¹⁹ E. Rössler, *Phys. Rev. Lett.* **65**, 1595 (1990).
 - ²⁰ M. T. Cicerone, F. R. Blackburn, and M. D. Ediger, *J. Chem. Phys.* **102**, 471 (1995).
 - ²¹ M. T. Cicerone and M. D. Ediger, *J. Phys. Chem.* **97**, 10489 (1993).
 - ²² F. Fujara, B. Geil, H. Sillescu, and G. Fleischer, *Z. Phys. B.* **88**, 195 (1992).
 - ²³ A. M. Puertas, M. Fuchs, and M. E. Cates, *Phys. Rev. E* **67**, 031406 (2003).
 - ²⁴ A. M. Puertas, M. Fuchs, and M. E. Cates, *Phys. Rev. Lett.* **88**, 098301 (2002).
 - ²⁵ A. M. Puertas, M. Fuchs, and M. E. Cates, *J. Chem. Phys.* **121**, 2813 (2004).
 - ²⁶ W. P. Krekelberg, V. Ganesan, and T. M. Truskett, *J. Chem. Phys.* **124**, 214502 (2006).
 - ²⁷ W. P. Krekelberg, V. Ganesan, and T. M. Truskett, *J. Phys. Chem. B* **110**, 5166 (2006).
 - ²⁸ Z. Yan, S. V. Buldyrev, N. Giovambattista, P. G. Debenedetti, and H. E. Stanley, *Phys. Rev. E* **73**, 051204 (2006).
 - ²⁹ A. B. de Oliveira, P. A. Netz, T. Colla, and M. C. Barbosa, *J. Chem. Phys.* **125**, 124503 (2006).
 - ³⁰ A. B. de Oliveira, P. A. Netz, T. Colla, and M. C. Barbosa, *J. Chem. Phys.* **124**, 084505 (2006).
 - ³¹ M. S. Shell, P. G. Debenedetti, and A. Z. Panagiotopoulos, *Phys. Rev. E* **66**, 011202 (2002).
 - ³² Y. Rosenfeld, *Phys. Rev. A* **15**, 2545 (1977).
 - ³³ Y. Rosenfeld, *J. Phys.: Condens. Matter* **11**, 5415 (1999).
 - ³⁴ M. Dzugutov, *Nature* **381**, 137 (1996).
 - ³⁵ P. G. Debenedetti, *Metastable Liquids. Concepts and Principles*. (Princeton University Press, 1996).
 - ³⁶ R. Yamamoto and A. Onuki, *Phys. Rev. Lett.* **81**, 4915 (1998).
 - ³⁷ M. D. Ediger, *Annu. Rev. Phys. Chem.* **51**, 99 (2000).
 - ³⁸ F. H. Stillinger and J. A. Hodgdon, *Phys. Rev. E* **50**, 2064 (1994).
 - ³⁹ G. Tarjus and D. Kivelson, *J. Chem. Phys.* **103**, 3071 (1995).
 - ⁴⁰ E. R. Weeks, J. C. Crocker, A. C. Levitt, A. Schofield, and D. A. Weitz, *Science* **287**, 627 (2000).